

See discussions, stats, and author profiles for this publication at: <https://www.researchgate.net/publication/40043443>

NBD-Based Green Fluorescent Ligands for Typing of Thymine-Related SNPs by Using an Abasic Site-Containing Probe DNA

ARTICLE *in* CHEMBIOCHEM · NOVEMBER 2009

Impact Factor: 3.09 · DOI: 10.1002/cbic.200900530 · Source: PubMed

CITATIONS

20

READS

35

5 AUTHORS, INCLUDING:



[Viruthachalam Thiagarajan](#)

Bharathidasan University

26 PUBLICATIONS 464 CITATIONS

[SEE PROFILE](#)



[Arivazhagan Rajendran](#)

Kyoto University

32 PUBLICATIONS 977 CITATIONS

[SEE PROFILE](#)

NBD-Based Green Fluorescent Ligands for Typing of Thymine-Related SNPs by Using an Abasic Site-Containing Probe DNA

Viruthachalam Thiagarajan,^[a, b, c] Arivazhagan Rajendran,^[a, d] Hiroyuki Satake,^[a, b] Seiichi Nishizawa,^[a, b] and Norio Teramae^{*[a, b]}

The binding behavior of green fluorescent ligands, derivatives of 7-nitrobenzo-2-oxa-1,3-diazole (NBD), with DNA duplexes containing an abasic (AP) site is studied by thermal denaturation and fluorescence experiments. Among NBD derivatives, *N*¹-(7-nitrobenzo[c][1,2,5]oxadiazol-4-yl)propane-1,3-diamine (NBD-NH₂) is found to bind selectively to the thymine base opposite an AP site in a DNA duplex with a binding affinity of $1.52 \times 10^6 \text{ M}^{-1}$. From molecular modeling studies, it is suggest-

ed that the NBD moiety binds to thymine at the AP site and a protonated amino group tethered to the NBD moiety interacts with the guanine base flanking the AP site. Green fluorescent NBD-NH₂ is successfully applied for simultaneous G>T genotyping of PCR amplification products in a single cuvette in combination with a blue fluorescent ligand, 2-amino-6,7-dimethyl-4-hydroxypteridine (diMe-pteridine).

Introduction

DNA-binding small molecules have attracted considerable attention for the development of drugs to control gene expression^[1] and they have also been used as important probes to detect specific sequences and lesion sites in DNA strands.^[2] Most of the DNA-binding ligands are either groove binders or intercalators,^[3] and such ligands have been used as a reporter molecules for the detection of single-nucleotide polymorphisms (SNPs) in combination with labeled or unlabeled probe DNAs.^[4] Because SNPs are responsible for the genetic variations associated with susceptibility to various common diseases and response to various drugs, a variety of methods have been developed to detect them, including high-density arrays, primer extension methods, and the Invader assay.^[4] Considering the future usage of the phenotype of each individual in personalized medicine and medical care,^[5] there is still a great demand for developing new typing methods that are high-throughput, high in accuracy, low in cost, and easy to operate.

Among the variety of methods for SNP typing, we have recently proposed a new noncovalent ligand-based fluorescence assay for SNP typing in combination with DNA duplexes containing an abasic or apurinic/apyrimidinic (AP) site.^[6] Related to the DNA-binding ligands and DNA lesions, Nakatani and co-workers reported specific recognition of a single guanine bulge by using 2-acrylamino-1,8-naphthyridines,^[7] and they have successfully demonstrated the selective detection of mismatched base pairs,^[8] SNPs,^[8a] and trinucleotide repeats,^[9] based on the binding of naphthyridine derivatives to the bulge sites in the DNA duplex by using surface plasmon resonance. In contrast, our method is based on the construction of a chemically stable AP site in a DNA duplex; this allows small synthetic ligands to bind to a target nucleotide, accompanied by fluorescence signaling. As shown in Scheme 1, an AP site-containing probe DNA is hybridized with a target DNA so as to


place the AP site toward a target nucleobase. In this way a hydrophobic microenvironment is provided for ligands to recognize the target nucleotide through hydrogen bonding; this is followed by π -stacking interactions between ligands and the bases flanking the AP site. Formation of hydrogen bonds between nucleobases and ligands at the AP site was confirmed by the appearance of imino protons in ¹H NMR spectra,^[6h, 10] and ³¹P NMR measurements revealed the interaction of a charged guanidinium moiety of amiloride with the phosphate backbone around the AP site.^[6d] Thermodynamic analysis based on isothermal titration calorimetry indicated that the

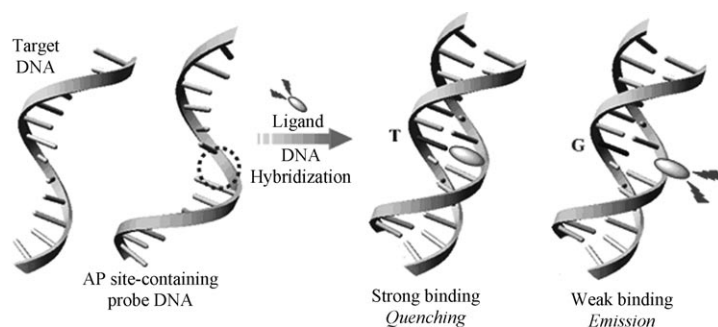
[a] V. Thiagarajan, A. Rajendran, H. Satake, S. Nishizawa, N. Teramae
Department of Chemistry, Graduate School of Science, Tohoku University
Aoba-ku, Sendai 980-8578 (Japan)
Fax: (+81) 22-795-6552
E-mail: teramae@mail.tains.tohoku.ac.jp

[b] V. Thiagarajan, H. Satake, S. Nishizawa, N. Teramae
CREST (Japan) Science and Technology Agency (JST)
Aoba-ku, Sendai 980-8578 (Japan)

[c] V. Thiagarajan
Present address: CEA
Institut de Biologie et Technologies de Saclay (IBITECS) and CNRS
Gif-sur-Yvette, 91191 (France)

[d] A. Rajendran
Present address:
Frontier Institute for Biomolecular Engineering Research (FIBER)
Konan University
7-1-20 Minatojima-minamimachi, Chuo-Ku, Kobe 650-0047 (Japan)

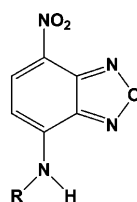
 Supporting information for this article is available on the WWW under <http://dx.doi.org/10.1002/cbic.200900530>: Fluorescence and UV-visible absorption responses of NBD-NH₂ for various target bases opposite the AP site, energy-minimized structures of the complexes between NBD-NH₂ and thymine, and the possible binding mode of NBD derivatives with T opposite the AP site.



Scheme 1. Schematic illustration of the ligand-based fluorescence detection of SNPs in combination with an AP site-containing DNA duplex.

hydrophobicity of a ligand was responsible for the increase in the binding affinity at the AP site.^[11]

We have successfully discovered a series of fluorescent ligands that can recognize a target nucleotide with high affinity and selectivity at an AP site in DNA duplexes; this series includes cytosine (C)-selective naphthyridine derivatives,^[6a,11] thymine (T)-selective amiloride^[6d] and riboflavin,^[10] guanine (G)-selective pteridine derivatives,^[6b,c] and adenine (A)-selective alloxazine.^[6f] By using G- and A-selective ligands, G > A genotyping was demonstrated in the analysis of PCR amplification products,^[6f] in which complexation-induced fluorescence quenching of alloxazine ($\lambda_{em} = 453$ nm) and 2-amino-6,7-dimethyl-4-hydroxypteridine (diMe-pteridine; $\lambda_{em} = 436.5$ nm) was utilized to detect the single base mutations. However, both of the above ligands show blue fluorescence, and the fluorescence detection for genotyping must be carried out by using a different cuvette for each ligand. To achieve the simultaneous detection of the multiple target bases in one cuvette, fluorescent ligands with different colors are necessary. Accordingly, green fluorescent 7-nitrobenzo-2-oxa-1,3-diazole (NBD) derivatives



NBD-NH₂: R = -CH₂-(CH₂)₂-NH₂

NBD-NMe₂: R = -CH₂-(CH₂)₂-N(CH₃)₂

NBD-C: R = -(CH₂)₂-CH₃

were chosen as new ligands for the detection of SNPs and their binding behavior was examined for nucleobases opposite an AP site in DNA duplexes. The green fluorescent probe NBD-NH₂ was found to bind selectively to the thymine target base over other nucleobases at the AP site with a binding affinity more than 10^6 M⁻¹, and the G > T genotyping of PCR amplification products was successfully demonstrated in a single cuvette by using NBD-NH₂ and diMe-pteridine as T- and G-selective ligands, respectively.

Results and Discussion

Thermal denaturation studies

First, we performed thermal denaturation experiments monitored by UV absorption at 260 nm as a function of temperature to examine the binding behavior of NBD derivatives with the AP site-containing DNA duplexes that contained various target nucleobases. Melting temperature (T_m) values were obtained by differentiating the melting temperature profiles by using eleven-mer DNA duplexes containing an AP site (5'-TCC AGX GCA AC-3'/3'-AGG TCN CGT TG-5', X = AP site (a propylene residue, Spacer C3), N = A, G, C, or T), and the results are summarized in Table 1. $T_{m(-)}$ and $T_{m(+)}$ denote the melting temperatures of

Table 1. Melting temperatures of AP-site-containing DNA duplexes in the absence and presence of NBD derivatives.

N	$T_{m(-)}$ [°C]		$T_{m(+)} (\Delta T_m)$ [°C]	
	without ligand	NBD-NH ₂	NBD-NMe ₂	NBD-C
T	27.4 ± 0.8	32.0 ± 1.0 (+4.6)	31.0 ± 1.0 (+3.6)	30.5 ± 0.8 (+3.1)
C	29.6 ± 0.9	32.0 ± 1.0 (+2.4)	32.0 ± 0.8 (+2.4)	31.6 ± 0.8 (+2.0)
A	33.5 ± 0.8	34.3 ± 0.1 (+0.8)	34.3 ± 0.3 (+0.8)	34.3 ± 0.6 (+0.8)
G	33.4 ± 0.7	34.2 ± 0.5 (+0.8)	32.8 ± 0.4 (-0.6)	33.9 ± 0.3 (+0.5)

DNA duplex is 5'-TCCAGXGCAAC-3'/5'-GTTGNCNCTGGA-3', where X is an AP site (Spacer C3) and N is T, C, A, or G. $T_{m(-)}$ and $T_{m(+)}$ denote the melting temperature in the absence and presence of NBD derivatives, respectively. Errors are the standard deviation obtained by four independent repeated measurements. [DNA duplex] = 20 μM, [ligand] = 100 μM in 2% DMSO, [NaCl] = 100 mM, [EDTA] = 1 mM, [sodium cacodylate] = 10 mM, pH 7.0.

DNA duplexes in the absence and presence of NBD derivatives, respectively. As can be seen in Table 1, in the absence of ligands, T_m values are low for pyrimidine bases (T and C) opposite the AP site in contrast to purine bases (A and G). This difference in T_m values can be ascribed to the intra- and extrahelical conformations of nucleobases opposite the AP site.^[12] Upon addition of ligands, a remarkable increase in the T_m value (ΔT_m) is observed for all ligands in cases in which T is the base opposite the AP site; this indicates the stronger binding of NBD derivatives with the DNA duplex containing a T target base. A moderate increase in T_m is observed for C, and the ΔT_m values for A and G are quite small. The ΔT_m values are in the order of T > C > A, G for all of NBD ligands. Among three NBD ligands, NBD-NH₂ gives the largest increase in T_m for T, and NBD-NMe₂ and NBD-C give moderate increases in T_m ; this suggests that the interaction between the tethered NH₂ group of NBD-NH₂ and a duplex containing an AP site is crucial for the strongest binding of NBD-NH₂. If a ligand binds to a fully matched DNA duplex through nonspecific intercalation or electrostatic interactions, then the T_m value of the DNA duplex (no AP site) will increase in the presence of the ligand.^[1b] We could not observe any significant change in T_m of the fully matched

DNA duplex in the presence of NBD-NH₂ (fully matched duplex: 5'-TCCAGGCAAC-3'/5'-GTTGCCCTGGA-3'; T_m (–) = 59.2 ± 0.3 °C; T_m (+) = 59.6 ± 0.5 °C; [DNA duplex] = 20 μM, [NBD-NH₂] = 100 μM). Accordingly, it can be regarded that the intercalation and electrostatic interactions do not take place in the present case.

Fluorescence experiments

The binding behavior of NBD derivatives with AP site-containing DNA duplexes was further examined by UV–visible absorption and fluorescence measurements by using 23-mer DNA duplexes (5'-GT GTGCGTTG CNC TGGACGCAGA-3'/5'-TCTGCG TCCA GXG CAACGCACAC-3'; X = spacer C3; N = G, C, A or T).

As shown in Figure 1, the fluorescence intensity of NBD ligands decreases upon addition of DNA duplexes containing an AP site without an appreciable shift in the emission maximum, whereas no significant changes in the fluorescence intensity are recognized upon addition of a DNA duplex which has no AP site (fully matched DNA duplex); this indicates that the

NBD moiety interacts solely with a target base opposite an AP site. The degree of fluorescence quenching of NBD derivatives is most remarkable in cases in which thymine is the target base and the strongest quenching is observed for NBD-NH₂ among three NBD ligands. To evaluate the binding affinity of NBD ligands with DNA duplexes containing thymine opposite the AP site, each ligand was titrated with the DNA duplex containing an AP site, and the resulting fluorescence titration curves (Figure 1D) were analyzed by a non-linear regression based on a 1:1 binding isotherm model.^[6a] The strongest affinity was obtained for NBD-NH₂ ((1.52 ± 0.07) × 10⁶ M^{–1}), and moderate and lower affinities were obtained for NBD-NMe₂ ((0.61 ± 0.02) × 10⁶ M^{–1}) and NBD-C ((0.14 ± 0.01) × 10⁶ M^{–1}); this order in the affinity is in accordance with the results of thermal denaturation experiments (Table 1) and the degree of fluorescence quenching (Figure 1A–C). By using NBD-NH₂ as a ligand, the differences in binding affinities for nucleobases opposite the AP site were examined by fluorescence titration experiments (Figure S2 in the Supporting Information). It was found that the binding affinity of NBD-NH₂ for T is about fivefold higher

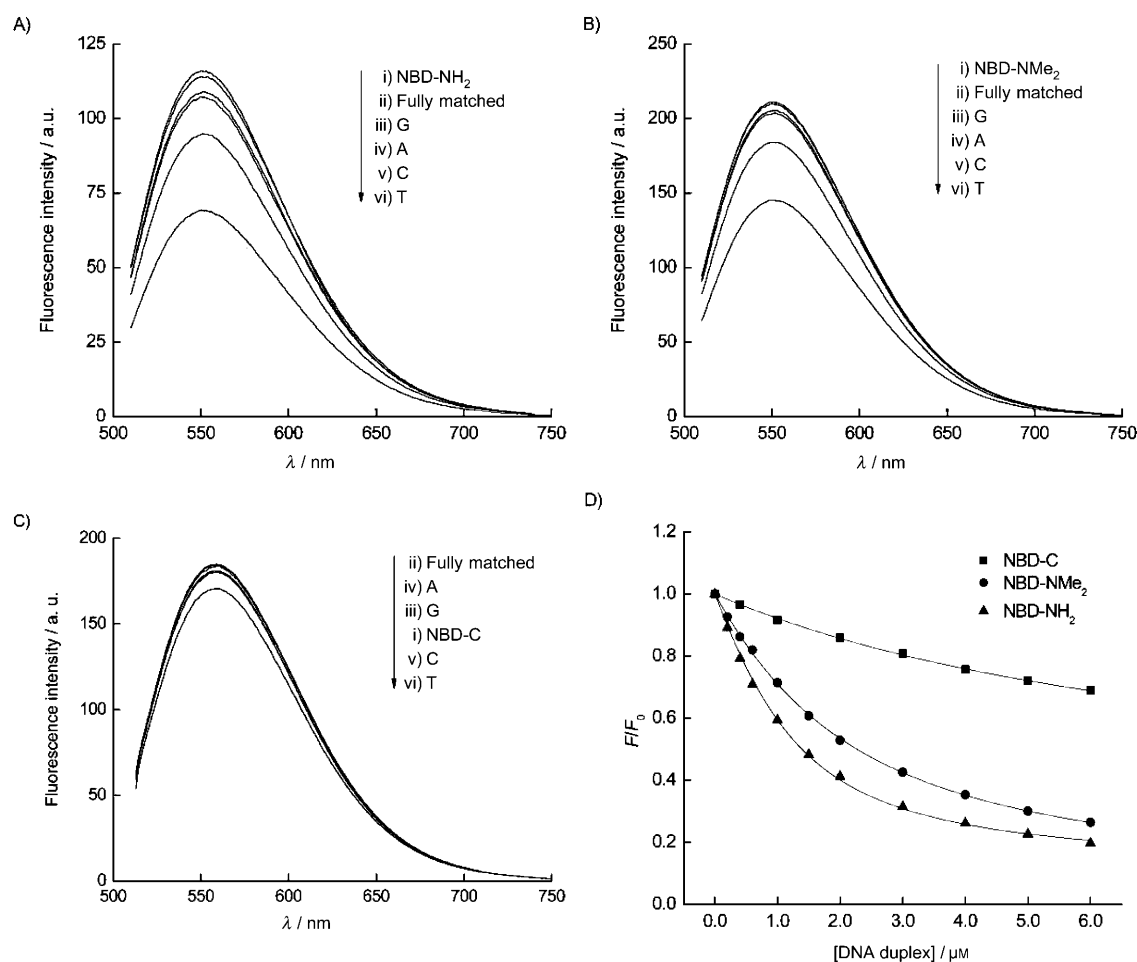


Figure 1. Fluorescence spectra of NBD ligands A) NBD-NH₂, B) NBD-NMe₂, C) NBD-C in the presence and absence of 23-mer DNA duplexes. i) and ii) in each figure denote, respectively, the fluorescence spectra of ligands without and with fully matched DNA. iii)–vi) denote the fluorescence spectra of ligands with AP site-containing DNA duplexes with G, A, C, and T target bases, respectively. D) Fluorescence titration curves for NBD ligands by addition of DNA duplexes containing T opposite the AP site. F and F_0 denote the fluorescence intensity with and without DNA duplexes. [ligand] = 1.0 μM, [NaCl] = 100 mM, [EDTA] = 1 mM, [sodium cacodylate] = 10 mM, pH 7.0, temperature 5 °C. DNA duplex = 5'-GTGTGCGTTG CNC TGGACGCAGA-3'/5'-TCTGCGTCCA GXG CAACGCACAC-3'; X = Spacer C3, N = G, A, C, or T. In fully matched DNA duplex, N = T and X = A. For A) to C) [DNA duplex] = 1.0 μM. For D) [DNA duplex] = 1.0 to 6.0 μM, λ_{ex} = 500 nm (isosbestic point) for NBD-NH₂ and NBD-NMe₂, λ_{ex} = 504 nm (isosbestic point) for NBD-C. Quartz cell (2 × 10 mm).

than C ($0.32(\pm 0.03) \times 10^6 \text{ M}^{-1}$) and more than tenfold higher than A ($0.15(\pm 0.02) \times 10^6 \text{ M}^{-1}$) and G ($0.08(\pm 0.03) \times 10^6 \text{ M}^{-1}$). Considering the difference in the binding affinities of NBD-NH₂ with nucleobases, NBD-NH₂ could be applicable to T>A and T>G genotyping. The order in selectivity (T>C>A>G) is also well reflected in the spectral changes of UV-visible absorption of NBD-NH₂ with and without DNA duplexes that have different nucleobases opposite an AP site (Figure S3). Upon addition of AP site-containing DNA duplexes, absorption intensity decreases and the absorption maximum shows a red-shift, which is due to the π -stacking interaction between NBD-NH₂ and bases flanking the AP site, with a clear isosbestic point at 500 nm; this wavelength was selected as the excitation wavelength for fluorescence measurements. Based on the high affinity and selectivity of NBD-NH₂ for the binding with T opposite an AP site in a DNA duplex, NBD-NH₂ can be expected to give sufficient fluorescence response for reliable discrimination of the T/G and T/A mutations, and the ligand can be applicable for the genotyping of PCR amplification products.

Ionic strength dependency of binding constants

Further, the binding behavior of NBD derivatives with DNA duplexes was studied by the ionic strength dependency of ligand–DNA binding affinities, by which thermodynamic parameters were obtained for the polyelectrolyte and nonelectrostatic components of overall binding free energy of ligand–DNA interactions.^[13] The binding affinity (K_{11}) was obtained from fluorescence titration experiments and its value was plotted against the salt concentrations (Figure 2). As shown in Figure 2, the binding constants for NBD-NH₂ and NBD-NMe₂ decrease remarkably as the salt concentration increases, while the decrease for NBD-C is quite less. According to the polyelectrolyte theory,^[13] an apparent charge on the ligand upon binding to the DNA duplex can be calculated from Equation (1):

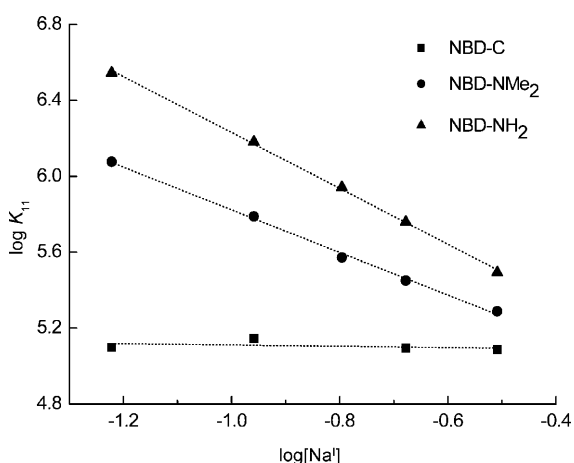


Figure 2. Salt dependence of binding constants for the interaction between NBD derivatives and DNA duplex containing thymine opposite an AP site. DNA duplex: 5'-GTGTGCGTTG CTC TGGACGCAGA-3'/5'-TCTGCGTCCA GXG CAACG CACAC-3'; X = spacer C3. [NaCl] = 60–310 mM, 5 °C.

$$SK = \frac{\partial \log K_{11}}{\partial \log [\text{Na}^+]} = -Z\Psi \quad (1)$$

in which SK is the slope of the linear least-squares analysis of $\log K_{11}$ vs. $\log [\text{Na}^+]$ plot, Z is the number of counterions released per ligand-binding event, which is equivalent to the apparent charge of the ligand, and Ψ is a constant equal to the fraction of counterions associated per phosphate (0.88 for B-type DNA^[14]). The apparent charges on NBD derivatives upon binding to DNA with a T target base were calculated as +1.67, +1.28, and +0.04 for NBD-NH₂, NBD-NMe₂, and NBD-C, respectively. The contribution of electrostatic interactions towards the total free energy was then calculated from Equation (2).^[13]

$$\Delta G_{\text{pe}} = -(SK)RT \ln [\text{Na}^+] \quad (2)$$

in which R is the gas constant and T is the absolute temperature. The polyelectrolyte (ΔG_{pe}) and nonelectrostatic (ΔG_{t}) contributions were examined from the overall binding free energy change ($\Delta G_{\text{obs}} = -RT \ln K_{11}$) by using Equation (3).^[13]

$$\Delta G_{\text{obs}} = \Delta G_{\text{pe}} + \Delta G_{\text{t}} \quad (3)$$

From the plots shown in Figure 2, polyelectrolyte and non-polyelectrolyte contributions to ΔG_{obs} were calculated and the dissected contributions are summarized in Table 2. It is re-

Table 2. Thermodynamic parameters for the binding of NBD derivatives to thymine in 23-mer DNA duplex containing an AP site.

NBD probes	$K_{11} \times 10^6$ [M ⁻¹] ^[a]	ΔG_{obs} [kcal mol ⁻¹]	Z	ΔG_{pe} [kcal mol ⁻¹]	ΔG_{t} [kcal mol ⁻¹]
NBD-NH ₂	1.52 ± 0.07	-7.86 ± 0.02	$+1.67 \pm 0.03$	-1.79 ± 0.03	-6.07 ± 0.04
NBD-NMe ₂	0.61 ± 0.02	-7.36 ± 0.02	$+1.28 \pm 0.04$	-1.37 ± 0.04	-5.99 ± 0.04
NBD-C	0.14 ± 0.01	-6.54 ± 0.05	$+0.04 \pm 0.06$	-0.04 ± 0.06	-6.50 ± 0.08

[a] K_{11} [M⁻¹] determined from fluorescence titration experiments by using a 1:1 binding isotherm model at 5 °C. ([sodium cacodylate buffer] = 10 mM; [NaCl] = 100 mM; [EDTA] = 1 mM, pH 7.0). ΔG_{obs} is the observed free energy change; Z is the apparent charge on the ligand upon complexation; ΔG_{pe} is the polyelectrolyte contribution to the observed free energy change; ΔG_{t} is the nonpolyelectrolyte contribution to the observed free energy change; DNA duplex: 5'-GTGTGCGTTG CTC TGGACGCAGA-3'/5'-TCTGCGTCCA GXG CAACGCACAC-3'; X = spacer C3. Errors denote the standard error.

vealed from the thermodynamic parameters listed in Table 2 that the nonpolyelectrolyte contribution is fundamental for the complexation of NBD derivatives with DNA duplex. It is also recognized that the polyelectrolyte contribution is large for protonated ligands, NBD-NH₂ and NMe₂ (NBD-NH₂: $-1.79 \text{ kcal mol}^{-1}$, NBD-NMe₂: $-1.37 \text{ kcal mol}^{-1}$), compared to a neutral ligand NBD-C ($-0.04 \text{ kcal mol}^{-1}$).

Molecular modeling: Molecular modeling was carried out with MacroModel Ver.9.0, considering the 1:1 complexation of NBD-NH₂ with a DNA duplex containing an AP site from a qualitative point of view. Although both the thymine base (T¹⁴)

opposite the AP site and the AP site adopted an extrahelical arrangement in the duplex containing an AP site (5'-C¹G²T³G⁴XG⁶T⁷G⁸C⁹-3'/3'-G¹⁰C¹¹A¹²C¹³T¹⁴G¹⁵T¹⁶G¹⁷C¹⁸-5', X = AP site)^[12] due to the stacking of G⁴ with G⁶, intercalation of an aromatic group conjugated to the DNA strand at the AP site was reported to form a single intrahelical form of a B-type DNA duplex^[15] by using the same sequence reported previously.^[12] By using a DNA duplex containing an AP site opposite thymine, an acridine derivative was reported to bind to the AP site by threading intercalation, and the acridine derivative stacked with the bases flanking the AP site keeping the intrahelical structure of the thymine base opposite the AP site.^[16] In our case, CD spectra of AP site-containing DNA duplexes with and without NBD-NH₂ show a couplet signal with a positive peak at around 280 nm and a negative peak at around 247 nm (Figure S4), similar to the CD spectrum of B-type DNA. Accordingly, a B-type conformation was adopted in the molecular modeling. Figure 3 shows the energy minimized model of the 1:1 com-

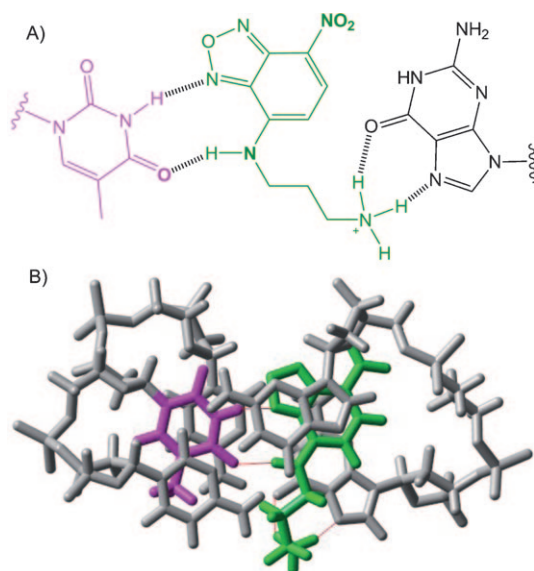


Figure 3. A) Possible binding mode of NBD-NH₂ with T opposite an AP site in a DNA duplex. B) Energy minimized structure obtained by MacroModel Ver. 9.0., for the complex between NBD-NH₂ and T opposite an AP site in a DNA duplex (5'-GTGTGCGTTG CTC TGGAC GCAGA-3'/5'-TCTGCGTCCA CAACGCACAC-3'; X = spacer C3). The NBD-NH₂ and the thymine base opposite the AP site are colored green and pink, respectively.

plex of NBD-NH₂ with the T target base opposite the AP site in a DNA duplex. The molecular modeling indicates that the formation of two hydrogen bonds is evident between NBD moiety and T, and that the tethered cation is oriented toward the major groove of the DNA duplex forming hydrogen bonds between the protonated amino group and the O6 and N7 atoms of guanine flanking the AP site. This structural feature is similar to the earlier studies^[17] in which the tethered ammonium ion is reported to direct toward the major groove and interact with electronegative atoms (N7 and O6) of guanine. This structural feature is also responsible for the strongest binding of NBD-NH₂ to the T target base opposite the AP site in a DNA duplex among three NBD derivatives. The nitrogen atom of an

N(CH₃)₂ group of NBD-NMe₂ can be protonated and charge-charge interaction can take place, whereas formation of one of hydrogen bonds between the protonated amino group and an O6 atom of guanine flanking the AP site is prevented as compared to NBD-NH₂. As for NBD-C, charge-charge interaction cannot be expected and only the NBD moiety contributes to the binding to the target T base. Thus the substituents govern the binding affinity of NBD derivatives with DNA duplexes containing an AP site (Figures S5 and S6).

Two-colored SNPs typing: Finally, NBD-NH₂ was applied to the detection of the G > T transversion present in codon 12 of the *K-ras* gene.^[18] Multicolor fluorescence is widely used in biosciences for simultaneous or sequential detection of multiple targets. We have recently demonstrated the G > A genotyping of PCR products of 107-mer DNAs (*K-ras* gene, codon 12) by using diMe-pteridine and alloxazine as G- and A-selective ligands, respectively.^[6f] Because the emission wavelengths of diMe-pteridine and alloxazine are similar (436.5 and 453 nm, respectively), a different cuvette containing a PCR amplification product must be used for each ligand to detect the G/A mutation by fluorescence. A mixture of fluorescent ligands that have different wavelengths of excitation (λ_{ex}) and emission (λ_{em}) would enable the multicolored typing of gene SNP sites simultaneously (Figure S7). First, 107-mer sense strands of the *K-ras* gene were amplified by asymmetric PCR as described in Experimental section. Then, an AP site-containing probe DNA is added into a single sample cuvette containing a PCR-amplified product of *K-ras* gene to form DNA duplexes. By the addition of a mixture of green fluorescent T-selective NBD-NH₂ ($\lambda_{ex}/\lambda_{em}$ = 474/550 nm) and blue fluorescent G-selective diMe-pteridine ($\lambda_{ex}/\lambda_{em}$ = 372/440 nm) into the cuvette, the type of alleles at a specific SNP site was determined by the fluorescence intensities of the T- and G-selective ligands at 550 nm and 440 nm, respectively.

Next, 24 samples of PCR amplification products (six G/G-homozygous, six T/T-homozygous, six G/T heterozygous, and six control solutions without PCR amplification product) were analyzed with a 20-mer probe DNA strand containing an AP site by using green fluorescent NBD-NH₂ and blue fluorescent diMe-pteridine ligands. Figure 4 shows the fluorescence intensity of the three genotypes in the *K-ras* gene, codon 12, fragment 107. Although the change in fluorescence intensity of NBD-NH₂ is not large compared to that of diMe-pteridine, SNP genotyping of the PCR amplification product samples, G/G, G/T, and T/T, can be clearly discriminated as three different clusters based on fluorescence responses of NBD-NH₂ (λ_{em} = 550 nm) and diMe-pteridine (λ_{em} = 440 nm). The control experiments measured without PCR product are located in the upper right corner and the plots are clearly separated from the other three clusters. These results indicate that the use of two different colored ligands in our assay allows the detection of both SNP alleles in a single cuvette, and three genotypes can be clearly distinguished from one another by measuring the intensity of blue and green fluorescence emission. The analysis requires no time-consuming steps such as purification of PCR amplification products and careful control of temperature, and the result could be readily obtained after PCR.

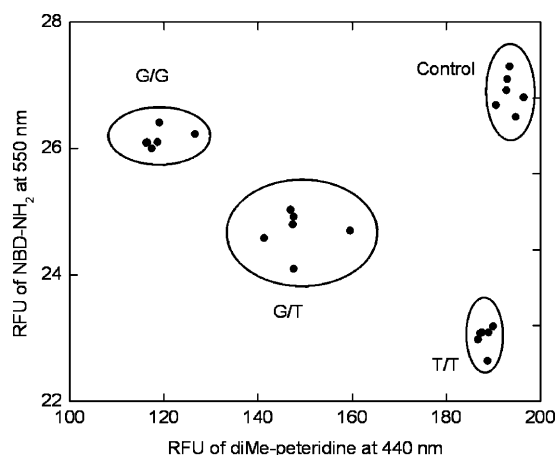


Figure 4. Scatter plots for G > T genotyping of 107-mer PCR products (*K-ras* gene, codon 12, sense strand) based on fluorescence responses of G-selective diMe-pteridine and T-selective NBD-NH₂. PCR product: 5'-GACTG AATAT AAAT TGTGG TAGTT GGAGC TGNTG GCGTA GGCAA GAGTG CCTG ACGAT ACAGC TAAAT CAGAA TCATT TTGTG GACGA ATAT GATCCA ACAATAG-3' (wild-type, N = G; mutant type, N = T); probe DNA: 5'-CCTACGCCAXCAGCTC-CAAC-3' (X = AP site, Spacer-C3). Temperature, 5 °C. Excitation and emission slit widths are 10 nm each. NBD-NH₂ (λ_{ex} = 474 nm; λ_{em} = 550 nm), diMe-pteridine (λ_{ex} = 372 nm; λ_{em} = 440 nm). Standard deviations are presented as ellipse.

Conclusions

In summary, we found that a green fluorescent ligand, NBD-NH₂, showed a highly selective and strong binding affinity for thymine opposite the AP site in DNA duplexes. The NBD-NH₂ probe was successfully demonstrated to be applicable for the simultaneous G > T genotyping of PCR amplification products in combination with a blue fluorescent ligand, diMe-pteridine. In the present genotyping, PCR amplification products could be readily analyzed by measuring fluorescence of added ligands without any pretreatment procedure.

Experimental Section

Materials: NBD derivatives were synthesized according to the literature.^[19] All of the oligodeoxynucleotides used in the present study were custom synthesized and HPLC purified (>97%) by Nihon Gene Research Laboratories Inc. (Sendai, Japan). For the synthesis of AP site containing DNAs, a propylene residue (Spacer phosphoramidite C3, Spacer C3) was utilized. The concentration of DNA was determined from the molar extinction coefficient at 260 nm.^[20] Water was deionized (≥ 18.0 M Ω cm specific resistance) by an Elix 5 UV Water Purification System and a Milli-Q Synthesis A10 system (Millipore Corp., Bedford, MA). The other reagents were commercially available analytical grade and were used without further purification.

Melting temperature (T_m) measurements: All measurements were performed in sodium cacodylate buffer solutions (10 mM, pH 7.0) containing NaCl (100 mM) and EDTA (1.0 mM). Concentrations of NBD derivatives and DNA duplexes were 100 and 20 μM , respectively. Before the T_m measurements, the sample solutions were annealed as follows: heated at 75 °C for 10 min, and then gradually cooled down to 5 °C (3 °C min⁻¹). Absorbance of DNAs was then

measured at 260 nm as a function of temperature by using an UV-visible spectrophotometer model 2450 (Shimadzu Corp., Kyoto, Japan) equipped with a thermoelectrically temperature-controlled micro multi-cell holder (eight cells; optical path length = 1 mm). The temperature ranged from 2–92 °C with a heating rate of 1.5 °C min⁻¹. The resulting absorbance versus temperature curves were differentiated to determine T_m values. Due to the poor solubility of NBD-C and NBD-NMe₂ in aqueous solution, all the melting temperature measurements (including NBD-NH₂) were carried out by using DMSO solutions (2%).

Fluorescence measurements: Fluorescence spectra of NBD derivatives were measured at 5 °C with a JASCO FP-6500 spectrofluorophotometer (Japan Spectroscopic Co. Ltd., Tokyo, Japan) equipped with a thermoelectrically temperature-controlled cell holder. All emission spectra were corrected for the instrumental spectral response. Sample solutions were buffered to pH 7.0 with sodium cacodylate (10 mM) containing NaCl (100 mM) and EDTA (1.0 mM). As described in the T_m measurements, the sample solutions were annealed before the fluorescence measurements. Due to the poor solubility of NBD-C and NBD-NMe₂ in aqueous solution, all the fluorescence studies for these two ligands were carried out by first dissolved in DMSO and further diluted by using an aqueous solution. The percentage of DMSO in the final assay volume is 0.005%. Binding constants (K_{obs}) of NBD-derivatives for the complexation with nucleobases in DNA duplexes containing an AP site were calculated by analyzing fluorescence titration curves with nonlinear least-squares regression based on a 1:1 binding isotherm.^[6a]

PCR procedures and Multicolor SNPs typing: A 107-mer *K-ras* gene^[16] (sense strand containing a codon 12 site) was amplified by asymmetric PCR (107-mer DNA: 5'-GACTG AATAT AAAT TGTGG TAGTT GGAGCTG (G/T) TGGCG TAGGC AAGAG TGCCT TGACG ATACA GCTAA TTCAG AATCA TTTTG TGGAC GAATA TGATC CAACA ATAG-3'; 0.5 ng). Eicosomer forward primer (5'-GACTGAATATAAAC TTGTGG-3' (300 pmol) and 20-mer reverse primer (5'-CTATT GTTGG ATCAT ATTCG-3'; 20 pmol) were added to 100 μL of the reaction mixture containing dNTPs (2.5 mM each), PCR buffer (10 \times , 10 μL ; TaKaRa), and Ex-Taq (2.5 U; TaKaRa). The thermal cycling program consisted of initial incubation at 94 °C for 5 min followed by 40 cycles of denaturation at 94 °C for 30 s, annealing at 52 °C for 30 s, and extension at 72 °C for 30 s, and then the sample was kept at 72 °C for 7 min. After thermal cycling and subsequent cooling to 4 °C, aliquots (40 μL) of the amplified DNA mixtures were buffered to pH 7.0 with sodium cacodylate (100 mM) containing EDTA (1.6 mM) and subsequently hybridized with AP site-containing 20-mer probe DNA (5.0 μM ; 5'-CCTAC GCCAX CAGCT CCAAC-3'; X = AP site). After hybridization, diMe-pteridine (0.1 μM) and NBD-NH₂ (0.1 μM) were added to the PCR mixture and fluorescence intensities were measured at both green- and blue-emission wavelengths.

Molecular modeling: Models of the 23-mer oligodeoxynucleotides and the NBD ligands were constructed by using Maestro 7.0. In order to construct the AP site in a 23-mer DNA duplex containing a thymine target base, the complementary adenosine unit was removed and a propylene residue was inserted between two phosphate moieties adjacent to the AP site. Molecular modeling was carried out with MacroModel Ver.9.0 (Schroinger, LLC, Portland, OR). After inserting ligands manually into the AP site, energy minimization was performed with Amber* force field and GB/SA continuum solvation model for water (with constant dielectric treatment for the electrostatic part) together with the default cut-off criterions; the gradient convergence threshold was set to be 0.005.

Acknowledgements

This work was partially supported by Grants-in-Aid for Scientific Research (A), No. 17205009, and Scientific Research (B), No. 18350039, from the Ministry of Education, Culture, Sports, Science and Technology, Japan. V.T. would like to thank the JST for a fellowship.

Keywords: abasic site • DNA recognition • DNA • fluorescence • single nucleotide polymorphism

- [1] See reviews and references herein: a) J. B. Chaires, *Curr. Opin. Struct. Biol.* **1998**, *8*, 314–320; b) R. Martinez, L. Chacón-García, *Curr. Med. Chem.* **2005**, *12*, 127–151; c) P. Palchaudhuri, P. J. Hergenrother, *Curr. Opin. Biotechnol.* **2007**, *18*, 497–503.
- [2] See reviews and references herein: a) P. B. Dervan, *Bioorg. Med. Chem.* **2001**, *9*, 2215–2235; b) S. Neidle, *Nat. Prod. Rep.* **2001**, *18*, 291–309; c) P. B. Dervan, B. S. Edelson, *Curr. Opin. Struct. Biol.* **2003**, *13*, 284–299.
- [3] See reviews and references herein: a) D. E. Graves, L. M. Velea, *Curr. Org. Chem.* **2000**, *4*, 915–929; b) S. M. Nelson, L. R. Ferguson, W. A. Denny, *Mutat. Res.* **2007**, *623*, 24–40.
- [4] See reviews and references herein: a) A.-C. Syvänen, *Nat. Rev. Genet.* **2001**, *2*, 930–942; b) K. Nakatani, *ChemBioChem* **2004**, *5*, 1623–1633; c) R. T. Ranasinghe, T. Brown, *Chem. Commun.* **2005**, 5487–5502.
- [5] a) F. S. Collins, E. D. Green, A. E. Guttmacher, M. S. Guyer, *Nature* **2003**, *422*, 835–847; b) W. Sadee, Z. Dai, *Hum. Mol. Genet.* **2005**, *14*, R207–R214; c) M. Hiratsuka, T. Sasaki, M. Mizugaki, *Clin. Chim. Acta* **2006**, *363*, 177–186; d) G. W. Duff, *Am. J. Clin. Nutr.* **2006**, *83*, 431S–435S.
- [6] a) K. Yoshimoto, S. Nishizawa, M. Minagawa, N. Teramae, *J. Am. Chem. Soc.* **2003**, *125*, 8982–8993; b) K. Yoshimoto, C.-Y. Xu, S. Nishizawa, T. Haga, H. Satake, N. Teramae, *Chem. Commun.* **2003**, 2960–2961; c) Q. Dai, C.-Y. Xu, Y. Sato, K. Yoshimoto, S. Nishizawa, N. Teramae, *Anal. Sci.* **2006**, *22*, 201–203; d) C. Zhao, Q. Dai, T. Seino, Y.-Y. Cui, S. Nishizawa, N. Teramae, *Chem. Commun.* **2006**, 1185–1187; e) B. Rajendar, Y. Sato, S. Nishizawa, N. Teramae, *Bioorg. Med. Chem. Lett.* **2007**, *17*, 3682–3685; f) B. Rajendar, S. Nishizawa, N. Teramae, *Org. Biomol. Chem.* **2008**, *6*, 670–673; g) Z. Ye, B. Rajendar, D. Qing, S. Nishizawa, N. Teramae, *Chem. Commun.* **2008**, 6588–6690; h) N. B. Sankaran, Y. Sato, F. Sato, B. Rajendar, K. Morita, T. Seino, S. Nishizawa, N. Teramae, *J. Phys. Chem. B* **2009**, *113*, 1522–1529; i) B. Rajendar, A. Rajendran, Y. Sato, S. Nishizawa, N. Teramae, *Bioorg. Med. Chem.* **2009**, *17*, 351–359.
- [7] K. Nakatani, S. Sando, I. Saito, *J. Am. Chem. Soc.* **2000**, *122*, 2172–2177.
- [8] a) K. Nakatani, S. Sando, I. Saito, *Nat. Biotechnol.* **2001**, *19*, 51–55; b) K. Nakatani, A. Kobori, H. Kumasawa, Y. Goto, I. Saito, *Bioorg. Med. Chem.* **2004**, *12*, 3117–3123; c) S. Hagihara, H. Kumasawa, Y. Goto, G. Hayashi, A. Kobori, I. Saito, K. Nakatani, *Nucleic Acids Res.* **2004**, *32*, 278–286; d) A. Kobori, S. Horie, H. Suda, I. Saito, K. Nakatani, *J. Am. Chem. Soc.* **2004**, *126*, 557–562.
- [9] K. Nakatani, S. Hagihara, Y. Goto, A. Kobori, M. Hagihara, G. Hayashi, M. Kyo, M. Nomura, M. Mishima, C. Kojima, *Nat. Chem. Biol.* **2005**, *1*, 39–43.
- [10] N. B. Sankaran, S. Nishizawa, T. Seino, K. Yoshimoto, N. Teramae, *Angew. Chem.* **2006**, *118*, 1593–1598; *Angew. Chem. Int. Ed.* **2006**, *45*, 1563–1568.
- [11] Y. Sato, S. Nishizawa, K. Yoshimoto, T. Seino, T. Ichihashi, K. Morita, N. Teramae, *Nucleic Acids Res.* **2009**, *37*, 1411–1422.
- [12] a) P. Cuniassé, G. V. Fazakerly, W. Guschlbauer, B. Kaplan, L. C. Sowers, *J. Mol. Biol.* **1990**, *213*, 303–314; b) J. T. Stivers, *Nucleic Acids Res.* **1998**, *26*, 3837–3844.
- [13] M. T. Record, C. F. Anderson, T. M. Lohman, *Q. Rev. Biophys.* **1978**, *11*, 103–178.
- [14] M. T. Record, R. Spolar in *The Biology of Nonspecific DNA–Protein Interactions* (Ed.: A. Revzin), CRC, Boca Raton, **1990**, pp. 33–69.
- [15] M. P. Singh, G. G. Hill, D. Peoc'h, B. Rayner, J.-L. Imbach, J. W. Lown, *Biochemistry* **1994**, *33*, 10271–10285.
- [16] A. Martelli, M. Jourdan, J.-F. Constant, M. Demeunynck, P. Dumy, *Bioorg. Med. Chem. Lett.* **2006**, *16*, 154–157.
- [17] a) A. K. Todd, A. Adams, J. H. Thorpe, W. A. Denny, L. P. G. Wakelin, C. J. Cardin, *J. Med. Chem.* **1999**, *42*, 536–540; b) B. Gold, *Biopolymers* **2002**, *65*, 173–179.
- [18] J. L. Bos, *Mutat. Res.* **1988**, *195*, 255–271.
- [19] a) S. Fery-Forgues, J.-P. Fayet, A. Lopez, *J. Photochem. Photobiol. A* **1993**, *70*, 229–243; b) A. Cotte, B. Bader, J. Kuhlmann, H. Waldmann, *Chem. Eur. J.* **1999**, *5*, 922–936; c) M. Onoda, S. Uchiyama, T. Santa, K. Imai, *Luminescence* **2002**, *17*, 11–14.
- [20] J. D. Puglisi, I. Tinoco, *Methods Enzymol.* **1989**, *180*, 304–325.

Received: August 24, 2009

Published online on November 30, 2009